Satellite-based estimation of mediterranean shrubland structural parameters

J. M.C. Pereira, T. M. Oliveira and J. C.P. Paul

Departamento de Engenharia Florestal, I.S. Agronomia
Tapada da Ajuda P-1399 Lisboa
Portugal

ABSTRACT

The potential of using Landsat TM5 imagery for determining biomass, percent canopy cover, and canopy volume of shrub fuelbeds was investigated by comparing field measurements with satellite spectral data. Twelve square sample plots were georeferenced with the aid of a global positioning system and differentially corrected for higher location accuracy. Differential illumination effects present in the imagery due to rugged topography were reduced using a digital terrain model.

Regression equations between ground data and satellite data were developed and the results extrapolated to the shrublands at Parque Natural das Serras de Aire e Candeeiros (PNSAC), in central Portugal. Best results were obtained using NDVI to estimate plot vegetation biomass (r^2=0,76), followed by canopy cover (r^2=0.65), and canopy volume (r^2=0.51). The ultimate aim of this ongoing project is the development of satellite-based fuel mapping capabilities, in order to support the application of spatially distributed fire behavior simulation models.

1. INTRODUCTION

Vegetation fires are a major problem in Portugal, where a total of approximately 1260000 hectares of forest, shrublands and rangelands (ca.14 % of the total area of the country) burned during the last 15 years. A Mediterranean-type climate, with warm, dry summers throughout most of the country is partially responsible for the extent and severity of the fire problem. Demographic and socio-economic changes in rural areas of the country, especially during the last 20-30 years represent another set of very influential factors. Since the early 1960's many of these areas have suffered moderate to severe population losses, due to internal migration to coastal cities, as well as emigration to wealthier countries, in Europe and America. These losses affected primarily the working-age population, leaving behind the very young and the old. Traditional economic activities, such as agricultural and livestock production declined, but local investment of the migrant worker's savings allowed for some local development.

Such changes drastically reduced traditional vegetation fuel use. Leaf litter, dead downed wood, and undergrowth shrubs used to be important sources of fuel for domestic consumption. Shrub biomass was also abundantly used to cover the floor of livestock enclosures, and then input to agricultural fields as fertilizer. Disruption of this dependence due to increased availability of electric power and industrial fertilizers led to progressive accumulation of high fuel loading in rural landscapes and is often mentioned as an important determinant of increased fire frequency and severity (Silva, 1990; Almeida and Moura, 1992; Rego, 1992).

The severity of the problem has led to the development of a series of research efforts, dealing namely with fuel mapping and fire spread simulation. The objective of the work reported in this paper, which is part of an ongoing research project, is the satellite-based mapping of structural properties of shrubland fuels relevant for fire spread simulation. Mapping of quantitative, biophysical vegetation parameters, such as biomass, canopy height and volume, or percent cover relies on the development of models relating these properties with satellite spectral data, possibly in the form of a vegetation index. In the initial stage of this project we are concentrating on developing simple empirical models relating vegetation parameters with Landsat TM5 spectral data.

1.1. Study area

The study area selected for shrubland fuel mapping is the Serras de Aire e Candeeiros Natural Park (PNSAC), in central-western Portugal. The Park covers an area approximately 37000 ha., ranging in elevation from 50m to 680m. and is located in a region of karstic geology. The area has a mean annual temperature of 14.8°C and a mean annual precipitation of 846 mm. Shrub formations are the dominant land cover type in the steeper slopes and hilltops, while agriculture occupies the more fertile *terra rossa* soils, in the valleys. Sheep and goat herding are practiced in the pastures of the main plateau between the two "Serras", and forest stands are more abundant at the base of the slopes. Natural vegetation is dominated by associations of the *Quercion broteroi* alliance and abundant *Quercus coccifera* formations result from degradation of forest cover. Concurrent action of fire and grazing lead to frequent presence of species typical of *Cisto-Lavanduletea* class, alternating with the *Calluno-Ulicetea* and the *Ononido-Rosmarinetea* classes (Espírito-Santo *et al.*, 1988).

Vegetation fires are a common element of the Park ecology, and are often used as a management tool to control the development of shrubs in pasturelands. Sometimes fire gets out of control and burns more extensively than intended, especially if it reaches areas of heavy shrub fuel loading on steep slopes. PNSAC management recognizes the need for more information on fire ecology of the Park and has provided both financial and logistic support to research described herein.

2. METHODS

2.1. Field-based vegetation analysis

Vegetation sampling and analysis took place in two stages. During the first stage, we performed dimensional analysis on 53 plants belonging to the 10 shrub species more abundant at PNSAC (**Table 1**).

Table 1 - Plant species and number of individuals used to develop dimensional analysis model for estimation of individual plant biomass (eq. 4)

Plant species	# plants
Quercus coccifera	5
Phyllirea angustifolia	5
Rosmarinus officinalis	8
Pistacia lentiscus	2
Cistus salvifolius	5
Cistus albidus	8
Lavandula luisieri	8
Arbutus unedo	2
Ulex parviflorus	2
Daphne gnidium	8

Stands where each species is abundant or dominant were located, and a stratified random design was used for individual plant selection. Sampling strata were defined based on plant height and diameter, and individual plants were selected by walking a random number of paces into the stand, in a randomly chosen azimuth. For each species, the plant located nearest to the stoping point was selected. The procedure was repeated until we obtained a sample size considered representative of the specific and structural composition of the shrublands. Plant height, diameter at 25 cm. height increments from the ground, and maximum diameter were measured in the field, then plants were cut, weighed and bagged for more detailed analysis. In the laboratory, we determined branch biomass in 1, 10 and 100-hour timelag (HTL) classes (Fosberg, 1970) and foliar biomass. Plant parts were oven-dried at 90°C (24 hours for leaves and 1-HTL branches; 48 hours for 10 and 100 HTL fuels) for dry weight calculation. These data were used to develop a regression model for estimating the total biomass of individual plants, with the simple dimensional measurements mentioned above as independent variables.

The second stage of vegetation analysis involved estimating biomass (fuel loading, ton.ha^{-1}), in 12 large square field plots, adequately located to cover a wide range of variation in vegetation abundance. Eight of the 12 plots measured 120 m on the side, and 4 measured 90 m. on the side, corresponding respectively to 16 and 9 Landsat pixels. The 12 plots were georeferenced with a global position system, by measuring the coordinates of the 4 corners. The positions were differentially corrected to a positional accuracy of 2-5 m. with data from a base station located 45 km southeast of PNSAC. The plots were meant to be internally homogeneous and placed within large patches of shrub formations, and at least 50 m. away from areas of different land cover types, such as roads, forest stands, fire scars, etc. in order to minimize the adjacency effect and consequences of possible georeferencing or registration errors.

Each plot was inventoried for biomass with 6 regularly spaced line transects, 3 with north-south orientation and 3 with east-west orientation, and 36 inventory points were located on a regular grid supported by these transects. Shrub plants found at each inventory point were measured for the same variables described above, and the data input into the dimensional analysis regression model, for biomass estimation. Whenever an inventory point fell on a non-vegetated spot, it was moved to nearest plant along the transects, with 5 m. spacing for the larger plots, and 3 m. spacing for the smaller plots, and plot canopy volume was calculated as the product of average vegetation height by percent cover. All field work was performed between April and July 1993.

Table 2 - Structural parameters and vegetation index values for the 12 field plots

Plot number	Mean height (m)	Canopy cover (%)	Canopy voulme ($m^3.m^{-2}$)	Biomass ($ton.ha^{-1}$)	NDVI
1	0.79	0.69	0.54	8.67	0.53
2	0.48	0.77	0.37	7.13	0.42
3	0.42	0.58	0.24	5.29	0.33
4	0.43	0.77	0.33	5.70	0.44
5	0.48	0.59	0.28	5.76	0.37
6	0.46	0.63	0.29	5.87	0.33
7[1]	0.37	0.49	0.18	4.34	0.37
8	0.36	0.89	0.32	10.04	0.59
9	0.33	0.24[2]	0.08	1.78	0.30
10[1]	0.60	0.67	0.40	7.00	0.48
11[1]	0.41	0.70	0.29	7.25	0.46
12[1]	0.47	0.69	0.32	4.40	0.42

[1] 90m by 90m plots.

[2] Plot 9 has 16 % of herbaceous vegetation cover, for a total green vegetation canopy cover of 40 % (see Discussion).

2.2. Spatial database development and satellite image processing

The spatial database developed for PNSAC includes a digital terrain model (DTM) and a Landsat TM5 image with all 7 channels. The DTM was digitized in-house, from 1:25000 topographic maps developed by the Portuguese Army Cartography Service. All 10 m. contour lines were digitized and the resulting vector file was rasterized to a 30 m cell size, for integration with the Landsat imagery. The TM imagery was geometrically corrected using control points obtained from the topographic maps and co-registered with the DTM using a linear polynomial and a nearest-neighbor resampling procedure, in order to preserve radiometric integrity of the data.

A simple analysis of TM visible channels histograms, according to the procedure of Chavez (1988) indicated that the imagery was gathered under a very clear atmosphere. Therefore, we considered it adequate to calculate the normalized difference vegetation index (NDVI) using apparent, or top-of-the-atmosphere (TOA) reflectance values of TM channels 3 (red) and 4 (infrared). The equation for apparent reflectance is (Markham and Barker, 1986; Moran *et al.*, 1992):

$$\rho_{ap} = \pi.\ L_{\lambda}) / (E_{o\lambda}.\cos_i.\ E_c), \text{ where:} \quad (1)$$

ρ_{ap} = dimensionless TOA reflectance.

L_{λ} = spectral radiance at the satellite sensor ($W.m^{-2}.sr^{-1}.\mu m^{-1}$).

$E_{o\lambda}$ = mean solar exoatmospheric irradiance ($W.m^{-2}.sr^{-1}.\mu m^{-1}$).

$\cos_i$ = cosine of the angular exoatmospheric of the direct solar flux onto the surface of each DTM pixel.

E_c = Earth orbit eccentrcity correction factor (in astronomical units, Iqbal, 1983).

Image DN values were converted to radiance units using the calibration coefficients recommended by Markham and Barker (1986). Implementation of equation (1) required calculation of a map of $\cos_i$ values for the entire study area, according to the formula (Iqbal, 1983; Gratton *et al.*, 1993):

$$\cos_i = \cos S.\cos\theta_s + \sin S.\sin\theta_s.\cos(\phi_s - A), \text{ where:} \quad (2)$$

S = local terrain slope.

θ_s = solar zenith angle.

ϕ_s = solar azimuth angle.

A = local terrain aspect.

In order to evaluate eq. (2), it was necessary to derive slope and aspect maps from the study area DTM. Once ρ_{TOA} maps were available for TM channels 3 e 4, NDVI was calculated according to the well known expression:

$$NDVI = (TM4 - TM3) / (TM4 + TM3) \quad (3)$$

Vector files containing the vegetation plot coordinates were then imported into the GIS (**figure 1**) and rasterized.

An average NDVI value was calculated for each of the 9 or 16 plot pixels and used as the independent variable in the regression equation for predicting shrubland biomass. Since the equation is only valid for shrublands, other land cover types were masked out in the Park NDVI image using land cover data obtained by digitising a vegetation map of the study area.

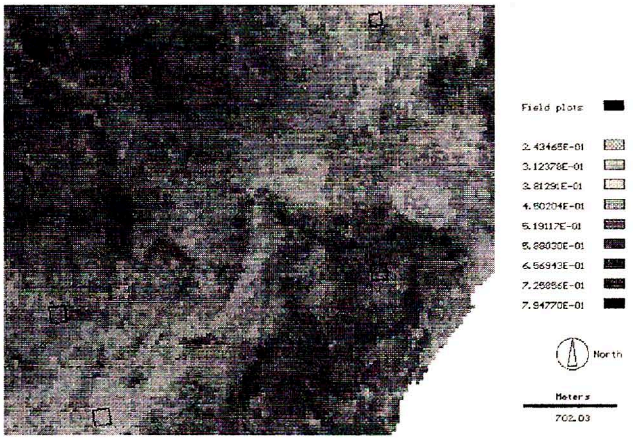

Figure 1 - NDVI image window from the Serra d'Aire, on the SE edge of PNSAC, showing range of NDVI values and placement of 4 of the 12 field plots

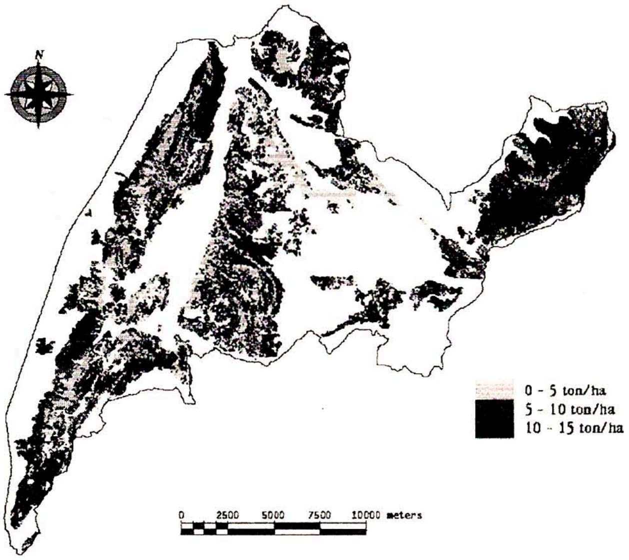

Figure 3 - Map of PNSAC showing shrublands and respective fuel loadings, in tons of biomass per hectare

3. RESULTS

The dimensional analysis of individual plant data yielded the following equation for biomass estimation from height and diameter measurements:

$Bio_{ind} = 0.642 * H^{0.0075} * D_{max}^{2.4901}$ (R^2= 0.91), where: (4)

Bio_{ind} = individual plant biomass (kg)
H = plant height (m)
Dmax = plant maximum diameter (m)

The model was adjusted with the module NONLIN of Systat5 for Windows (reference), using the Quasi-Newton algorithm. Asymptotic standard errors for the parameter estimates are 0.046 for the constant term, 0.142 for the exponent of variable H, and 0.168 for the exponent of variable D_{max}. The biomass estimates obtained with equation 4 were used in the inventory procedure described in section 2.1 to calculate plot biomass. Paúl (1993) determined the percent standard error of the mean for the plot-level biomass estimates and found values ranging from 12 % to 44 %. For 6 of the plots the error is smaller or equal than 15 %, and only for 3 plots is the error larger than 30 %. These estimates were correlated with mean plot NDVI (**Figure 2a**). The regression model represented in **Figure 2a** is given by:

$Bio_{plot} = -2.923 + 21.486 * NDVI$ (R^2=0.76), where (5)
Bio_{plot} = plot biomass (ton.ha^{-1}).

Standard error of the parameter estimates for equation 5 is 1.657 for the intercept and 3.87 for the slope.

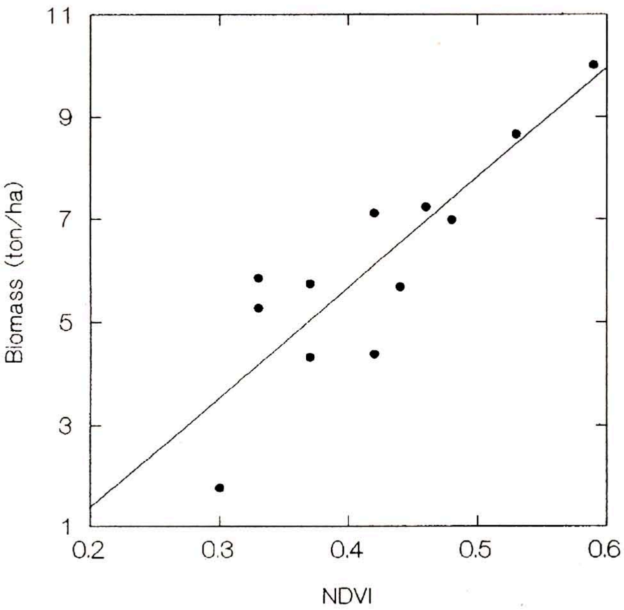

Figure 2 - NDVI vs. plot vegetation structure scatterplots. a) NDVI vs. biomass

Figure 3 displays a map of shrub fuel loading classes for PNSAC, where shrubland areas were identified with the digital land cover map mentioned above, and fuel loadings were obtained from equation 5. NDVI was also used to estimate percent canopy cover and canopy volume, per plot. The equation relating NDVI with canopy cover is **(Figure 2b)**:

$\%cover_{plot} = 1.211 + \log(NDVI^{0.641})$ (R^2=0.65), where (6)
$\%cover_{plot}$ = plot canopy cover (%).

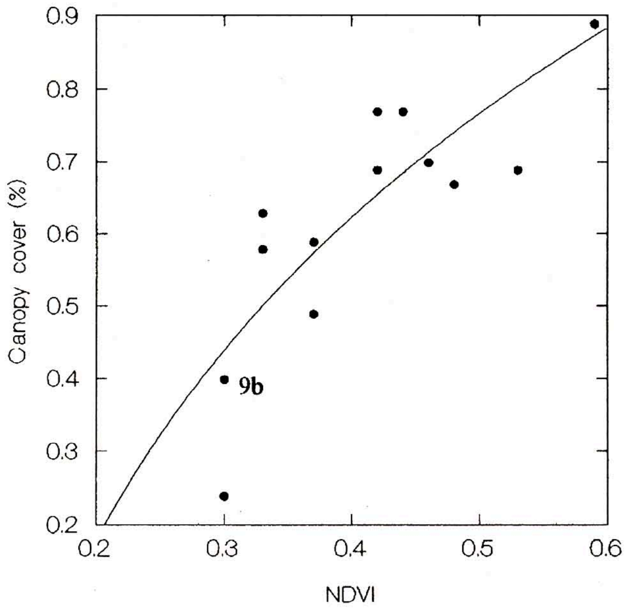

Figure 2b - NDVI vs. canopy cover. Plot 9b has 24 % of shrub cover and 16 % of herbaceous cover. Straight below 9b is plot 9, which represents the same location, but considering only shrub cover (see Table 2 and Discussion)

Asymptotic standard error of the parameter estimates for equation 6 is 0.16 for the constant term and 0.375 for the exponent. The relationship between NDVI and canopy volume is given by **(figure 2c)**:

$canvol_{plot}$ = -0.088 + 0.932 * NDVI (R^2=0.51), where (7)
$canvol_{plot}$ = plot canopy volume ($m^3.m^{-2}$).

Standard error of the parameter estimates for equation 7 is 0.123 for the intercept and 0.287 for the slope.

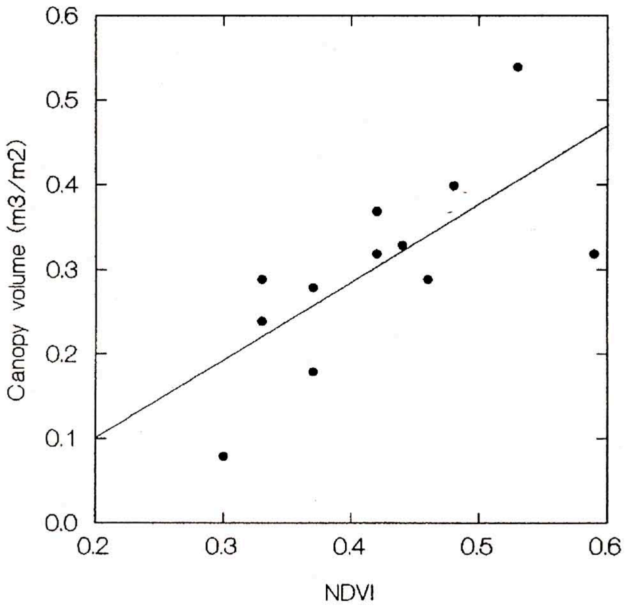

Figure 2c - NDVI vs. canopy volume. See Discussion for comments on plot 8, the one with the highest NDVI value

4. DISCUSSION

Estimation of plant biomass at the plot level was performed as the two-stage process described in section 2.1. There are, therefore, two main sources of error for these estimates: the estimation of individual plant biomass, and extrapolation of these estimates to the entire plot. Goodness-of-fit statistics given for equation 4, and the more thorough analysis by Paúl (1993), presenting predictive ability and multicollinearity statistics for this model, indicate that it fits the data very well, has good predictive ability and low collinearity. Paúl (1993) also assessed the adequacy of pooling plants from all species into a single regression model by testing for significance of differences between regression coefficients of the overall model and those of models containing smaller groups of species, and concluded that global pooling was an acceptable procedure. The magnitude of percent standard error of the mean values for the plot-level biomass estimates indicate that it would be adequate to increase sampling intensity above the current level of 36 points per plot.

Of the shrubland structural attributes determined at the level of the plot and correlated with NDVI, biomass has the best fit, followed by % cover. The weakest correlation is with canopy volume. Biomass per unit area is the most important stand characteristic for fuel modelling and fire behavior simulation, and therefore the results are encouraging. The relationship between NDVI and biomass seems to be linear, for the range of biomass amounts present in the study area. However, various authors have noticed an asymptotic trend in the relationship between leaf area index (LAI) and vegetation indices, for values of LAI larger than about 3 (Peterson *et al.*, 1987; Baret et Guyot, 1991). This trend may, therefore, occur at sites with higher fuel loadings and create difficulties for fuel mapping based on vegetation indices.

The correlation between NDVI and canopy cover takes a non-linear form **(figure 2b)** essentially due to plot 9, which has the lowest levels of shrub canopy cover and mean vegetation height of all 12 plots, probably due to the fact that it was located in a relatively recent fire scar. An higher than expected NDVI value may be explained by the presence of a much higher proportion of herbaceous vegetation cover than at any other plot (16 %, compared to 4 % for the next higher level of herbaceous cover, which is virtually absent from 9 of the plots (Paúl, 1993). Thus, in equation 6, herbaceous vegetation contributes to NDVI but not to the corresponding value of canopy cover, since this refers only to shrubby vegetation. If herbaceous and shrub cover are added, the total green vegetation cover of plot

9 goes up to 40 %, as shown by the data point labeled 9b in **Figure 2b**. The relationship between the two variables loses its non-linear character and can be fitted by a straight line with $R^2 = 0.64$ (not shown). The biomass of plot 9 herbaceous vegetation is quite small, and therefore the effect discussed here seems to be absent from the relationship between NDVI and biomass.

The relatively poor fit between NDVI and canopy volume is primarily due to plot 8, which has the highest fuel loading and shrub canopy cover of all plots, but a quite low mean vegetation height. The strongly dominant shrub species at this plot is *Ulex parviflorus*, a species that tends to have bulk density values on the high range, for the species studied at PNSAC (Paúl, 1993; Pereira *et al.*, to appear) and usually grows in tight, continuous stands. This contrasts somewhat with the spatial arrangement of plants in most other shrub formations of the study area, where individual crowns tend to be farther apart. The idiosyncratic canopy architecture of *U. parviflorus* dominated stands, may thus be responsible for the outlier behavior of plot 9, which has a strong influence on a regression model with only 12 observations.

Figure 3 shows the spatial distribution of shrub biomass, or shrub fuel loadings at PNSAC. Areas of very high loadings (10-15 tons/ha) can be found in small patches scattered throughout the Park, and usually associated with drainage features. Intermediate levels of fuel loading (5-10 tons/ha) are particularly abundant at Serra d'Aire, on the eastern edge of the Park, but can also be found in smaller patches at the westernmost Serra dos Candeeiros and in the central plateau. Lower fuel loadings (0-5 tons/ha) predominate in areas of more intensive sheep and goat herding in the central plateau, and around agricultural valleys. The very fine-grained mosaic revealed by Figure 3 reflects the underlying heterogeneity of the natural environment and cultural practices, but it is also, to some extent, an artifact of the discretization of a continuous variable into 3 classes.

5. CONCLUSIONS

Based on our results, it seems possible to estimate structural parameters of mediterranean shrublands with a degree of accuracy adequate for large scale fuel modelling and mapping. The current methodology can be improved, however, and we are developing a new vegetation structure sampling procedure based on the use of a portable field spectroradiometer and small (1-4m^2) plots. These will be used for destructive analysis of vegetation and calibration of equations relating shrubland community structure with field spectroradiometric data. It will be possible to apply the same equations to Landsat TM radiometric data and obtain estimates of shrubland fuel loading and structure over broad geographic areas.

In the regression analysis of NDVI and canopy cover data, a deviant plot corresponds to an earlier post-fire seral stage than at other plots, when grasses are more abundant, and the outlying data point in the NDVI vs. canopy volume scatterplot represents a plot strongly dominated by a single shrub species of relatively high bulk density. These results reveal the confounding effects of canopy architecture, species composition and community diversity. In order to address these problems, the PNSAC data are being reanalysed with spectral mixture analysis models (Adams *et al.*, 1986; Smith *et al.*, 1990), in an attempt to improve our ability to discriminate between different ecological communities, and use the shade endmember to infer community physiognomy (Ustin *et al.*, 1993).

REFERENCES

Adams J.B., Smith M.O. & Johnson P.E., 1986, Spectral mixture modeling: a new analysis of rock and soil types at the Viking Lander I site. *Journal of Geophysical Research*, **91**: 8098-8112.

Almeida A.M.S.F. & Moura P.V.S.V., 1992, The relationship of forest fires to agro-forestry and socio-economic parameters in Portugal. *International Journal of Wildland Fire*, **2** (1): 37-40.

Baret F. & Guyot G., 1991, Potentials and limits of vegetation indices for LAI and APAR assessment. *Remote Sensing of Environment*, **35**: 161-173.

Chavez Jr., P.S., 1988, An improved dark-object subtraction technique for atmospheric scattering correction of multispectral data. *Remote Sensing of Environment*, **24**: 459-479.

Dozier, J. & Marks D., 1987, Snow mapping and classification from Landsat Thematic Mapper data. *Annals of Glaciology*, **9**: 97-103.

Espírito-Santo M.D., Lousã M.F., Costa J.C., Cortes P. & Monjardino J., 1988, Plantes endémiques et rares du Parc Naturel "Serras de Aire e CAndeeiros". Actes del Simposi International de Botânica Pius Font i Quer, vol. II *Fanerogâmica*, pp. 349-352, Barcelona.

Fosberg M.A., 1970, Drying rates of heartwood below fiber saturation. *Forest Science*, **16** (1): 57-63.

Gratton D.J., Howarth P.J. & Marceau D.J., 1993, Using Landsat-5 Thematic Mapper and digital elevation data to determine the net radiation field of a mountain glacier. *Remote Sensing of Environment*, **43**: 315-331.

Iqbal M., 1983, Introdution to Solar Radiation. Academic Press, New York.

Markham B.L. & Baker J.L., 1986, Landsat MSS and TM post-calibration dynamic ranges, exoatmospheric reflectances and at-satellite temperatures. *EOSAT Landsat Technical Notes*, **1**:3-8.

Moran M.S., Jackson R.D., Slater P.N. & Teillet P.M., 1992, Evaluation of simplified procedures for retrieval of land surface reflectance factors from satellite sensor output. *Remote Sensing of Environment*, **41**: 169-184.

Pereira J.M.C., Sequeira N.M.S. & Carreiras J.M.B., (to appear), Structural properties and dimensional relations of some mediterranean shrub fuels. *International Journal of Wildland Fire*.

Peterson D.L., Spanner M.A., Running S.W. & Teuber K.B., 1987, Relationship of Thematic Mapper simulator data to leaf area index of temperate coniferous forests. *Remote Sensing of Environment*, **22**: 323-341.

Rego F.C., 1990, Land use changes and wildfires. In: Responses of Forest Ecosystems to Environmental Changes (ed. A. Teller, P. Mathy, and J.N.R. Jeffers), Florence, Italy. Elsevier Applied Science, London.

Silva J.M., 1990, La gestion forestière et la sylviculture de prévention des espaces forestiers menacés par les incendies au Portugal. *Revue Forestière Française*, **40** (n° spécial): 337-345.

Smith M.O., Ustin S.L., Adams J.B. & Gillespie A.R., 1990, Vegetation in deserts. I. A regional measure of abundance from multispectral images. *Remote Sensing of Environment*, **29**: 1-26.

Ustin S.L., Smith M.O. & Adams J.B., 1993, Remote sensing of ecological processes: a strategy for developing and testing ecological models using spectral mixture analysis. In: Scaling Physiological Processes – Leaf to Globe (ed. J.R. Ehleringer and C.B. Field). Academic Press Inc., San Diego.